Military Technical College,
Kobry El-Kobbah,
Cairo, Egypt

9th International Conference
On Aerospace Sciences &
Aviation Technology

THE APPLICATION OF ACTUATOR DISKS TO THE CALCULATION OF NON-UNIFORM FLOWS IN TURBOFAN ENGINES

JOO* W.G.

ABSTRACT

One of the important issues in the assessment of the inlet/engine compatibility in turbofan engines is to predict the coupling effects between the non-uniform inlet and engine. The computational method using an actuator-disk model has been applied to the calculations of the flow through a civil high-bypass-ratio turbofan engine with drooped intake and the flow through a multistage turbofan engine subjected to non-uniform total pressure inlet flow. The results of a series of calculations are presented and the nature of the interactions between the flow through a fan and non-uniform inlet flow is addressed.

KEY WORDS

Actuator disk, Flow field interaction, Non-uniform flow, Turbofan engine

*Associate professor, Dpt. of Mechanical Engineering, Yonsei University, Seoul, Korea.

INTRODUCTION

Today, the basic trend in the design of a turbofan engine is to increase the engine bypass ratio to improve the propulsion efficiency. However, the increase of nacelle diameter necessary to obtain higher bypass ratios could produce an unacceptable drag penalty because of the additional wetted surface area, and increased weight. A possible solution, maintaining the benefit from an increase in the bypass ratio, is to use shorter and slimmer nacelles with low contraction ratio.

The principal problem associated with low contraction ratio intakes is the high level of flow distortion. Although the engine inlet is designed with the aim of providing satisfactory inlet conditions to an engine, it is difficult to avoid distortion due to internal separation while stationary, in crosswind or high incidence conditions, particularly in low contraction ratio intakes. This distortion can lead to high fan stresses and noise, a reduction in performance and more importantly a decrease in engine surge margin.

The response of a compressor to distorted flow can be divided into two major aspects: the redistribution of inlet flow approaching a blade row and the resulting change in the overall compressor performance. These two subjects are strongly coupled and cannot be considered separately since the change in overall compressor performance will affect the redistribution of inlet flow.

Many theoretical models [1] to predict flow field coupling effects between a compressor and inlet distorted flow have been developed, but most of them are two dimensional methods based on parallel compressor analysis or linearised theory, and the solution of three dimensional linearised equations [2-3] is found for only the case of steady incompressible linearised free vortex flow. These methods predict some important aspects in flow field coupling, but are difficult to use for the practical problems with complicated geometry.

Joo and Hynes [4] developed a three-dimensional computational method using actuator disk models of blade rows for the calculation of non-uniform flow with long length scale, which is capable of predicting non-uniform inlet flow and engine flow field coupling effects in a complicated turbofan geometry.

This paper investigate, with calculation results obtained using their method, the features of flow field interaction between single fan flow and non-uniform static pressure inlet flow due to the drooped intake in a typical modern high-bypass civil turbofan engine and flow field interaction between multistage fans and non-uniform total pressure inlet flow in a military multistage turbofan engine.

CALCULATION METHOD

The calculations of the non-uniform flow through blade row require a computation of the unsteady three-dimensional viscous flow through the whole annulus including all blade passages because the non-uniform flow does not satisfy the periodic boundary condition. This kind of calculations may be performed using a current available

supercomputer, but it is not practical for engineering purpose. This leads to a need to model the flow within the blade rows.

Any model for use in this context must comprise two parts: a method for calculating the flow fields outside blade rows and a reliable way of estimating fan performance in non-uniform flow. Flow fields calculation methods are reasonably well developed, but it is the estimation of fan performance that is more pressing issues.

A characteristic feature of the flow field asymmetry associated with intake, pylon, or non-uniform total pressure flow is that the circumferential length scales of interest are long when compared with a blade pitch. Most of the models applicable to low hub-to-tip ratio blade rows exploit this feature and use an actuator disk or a semi-actuator disk blade row model. The essential idea is that the local blade performance at each radius and at each circumferential location can be related to the performance that the blade would exhibit in clean flow when subjected to the same inlet conditions. Simple corrections to account for the effects can also be incorporated.

The present computational method is using an actuator disk blade row model and has been developed by Joo and Hynes [4]. The important issues related to an actuator disk model such as the sensitivity of solution to the disk location are described in details in Joo and Hynes [4] and thus a brief description of the method and the extra details relevant to the current calculation are given here.

Computational Method for Flow Field Regions

The flow fields outside blade are found from the solutions of three dimensional Reynolds averaged Navier-Stokes equations in conservation form. These equations are written in the absolute frame using a cylindrical coordinate system, because the distorted flow field is assumed to be steady in this frame.

$$\frac{\partial}{\partial t}\int_{\Omega} U d\Omega + \int_{A} \overline{F}\cdot\overline{dA} = \int_{\Omega} Q d\Omega \qquad (1)$$

where

$$U=\begin{bmatrix}\rho\\ \rho V_x\\ \rho V_\theta\\ \rho V_r\\ \rho E\end{bmatrix} \qquad \overline{F}=\begin{bmatrix}\rho\overline{V}\\ \rho V_x\overline{V}+\overline{\overline{\tau}}\,\overline{i_x}\\ r\rho V_\theta\overline{V}+r\overline{\overline{\tau}}\,\overline{i_\theta}\\ \rho V_r\overline{V}+\overline{\overline{\tau}}\,\overline{i_r}\\ \rho H\overline{V}\end{bmatrix} \qquad Q=\begin{bmatrix}0\\ 0\\ 0\\ \dfrac{\rho V_\theta^2+p}{r}\\ 0\end{bmatrix}$$

with

$\overline{V}=V_x\overline{i_x}+V_\theta\overline{i_\theta}+V_r\overline{i_r}$, Absolute velocity

$\overline{\overline{\tau}}=$ Stress tensor containing both the static pressure and viscous stresses

$E = c_v T + \frac{V^2}{2}$, Total internal energy

H = Stagnation enthalpy

Ω = Volume of the control volume

$\overline{A}$ = Areas of the control volume surface

These equations are discretised on a set of control volumes, formed by a simple, structured H-grid construction. Flow variables are stored at cell centers and values on cell faces for flux evaluation are thus found by a simple average of the cell variables on either side of the face with second-order accuracy on smoothly varying grids.

The size of grids near boundaries used for the calculation is usually too large in comparison with a boundary layer thickness to resolve annulus boundary layers. Therefore, only the laminar shear stress, not turbulence, is considered and the calculation would become effectively inviscid one. The discretised set of equations of motion is solved by time marching. The basic solution algorithm is the same as that developed by Dawes [5] for the calculation of the flow within a single blade row passage. This time marching scheme consists of a two-step explicit and one-step implicit scheme derived as a pre-processed simplification of the Beam-Warming algorithm.

Actuator Disk Boundary Conditions

The length scales that are likely to characterize the flow interactions between fans and intakes and downstream components are much larger than a blade pitch. In addition, it will emerge that some of the compatibility issues do not involve directly the flow within the blade rows themselves. In these circumstances an actuator disk model for a blade row would seem a useful first approximation.

The flow fields upstream and downstream of the blade row are coupled by boundary conditions imposed across the actuator disk to represent the fan performance. Five matching conditions are required across an actuator disk, corresponding to the five independent flow variables in the equations of motion. The boundary conditions used in the present model, which are applied at each radial location and at each circumferential position, are:

(i) conservation of mass,
(ii) conservation of radial momentum,
(iii) conservation of rothalpy,
(iv) relative exit flow angle specified,
(v) entropy rise (or total pressure change) specified.

The last two conditions are associated with blade performance, which are given as input data. The flow angle at exit to the actuator disk could be taken directly from the values of the measured or calculated flow angle at the blade trailing edge. The flow through the rotor subjected to the non-uniform inlet flow is unsteady to a certain extent, but this unsteady effect is assumed to be neglected.

The conditions described above must be modified when blade sections are choked, since this set of boundary conditions does not contain an allowance for blade blockage. In present calculations, a simple model for choking suggested by Joo and Hynes [4], based on two-dimensional flow into a choked blade section, was incorporated into the actuator disk boundary condition (i) and (v).

The way to integrate these actuator disk boundary conditions into a numerical model depends on the numerical scheme used for calculating flow field regions. The detailed implementation of actuator disk boundary conditions used in the present calculation can be found in Joo and Hynes [4].

Validation of Method

To validate the developed computational method and to investigate the effects of turbofan installations, Joo and Hynes [6] applied the method to calculations of the flow through the civil high bypass ratio turbofan engine and its installation. A cross section of calculation domain is shown in Fig.1. The engine has a droop simulator designed for taking account of the effect of a drooped intake at cruise. A fan and an outlet guide vane (OGV) in the bypass duct are contracted to plane actuator disks which are located at mid-chord of each blade row.

The flow fields upstream and downstream of the blade row are found using a fully three-dimensional computational method and coupled by boundary conditions imposed across the actuator disk to represent the blade row performance. The locations of the OGV actuator disk and the splitter are moved slightly towards the fan to keep the true actual gap distances between them and the fan.

The values of relative flow angles and losses at the exit to the fan actuator disk were obtained from a three dimensional viscous calculation (using BTOB3D) of the flow through the fan operating near design in uniform inlet flow. The radius of the annulus varies significantly through the fan blade row as shown in Fig.1. The work done by the fan disk, therefore, is influenced somewhat by the disk location if the true blade exit flow angles are used. In order to reproduce the correct work distribution the true flow angles are corrected slightly using an approximate method suggested by Joo and Hynes [4]. The OGV is assumed to turn the flow to the axial direction without deviation.

All components of the engine downstream of the fan, which are thought to affect the response of the fan, are also simulated. The calculation domain in the core engine section is extended to just upstream of the engine section stator (ESS) where a boundary condition simulating the presence of the core engine is imposed. The calculation domain in the bypass stream is continued around the pylon and the corresponding strut at bottom dead centre to a section well past the pylon leading edge.

The flow at the inlet boundary to the calculation domain is assumed to be non-swirling, to have uniform stagnation pressure and stagnation temperature and to be roughly aligned with the streamwise surfaces of the calculation grid.

At the outlet boundary located just upstream of the engine section stator (ESS) in the core engine section, a condition simulating the presence of the core engine is imposed. The pressure rise characteristics of the core engine are very steep when compared with that of the fan root and thus the core compressor will not accept much in the way of a circumferentially non-uniform reduced mass flow. A constant mass flow coefficient, $\frac{\dot{m}\sqrt{C_p T_0}}{AP_0}$, is, therefore, specified at each radius and circumferential position.

The outlet boundary in the bypass section is located at some distance downstream of the pylon leading edge and the corresponding strut leading edge at bottom. If the flow at outlet to the calculation domain is assumed to have no circumferential variation, the imposed boundary condition is usually the fixed hub or tip static pressure with the radial variation consistent with simple radial equilibrium. However, the static pressure variations present in the flow with strong flow field interaction have considerable low order circumferential harmonics which persist a long way downstream and thus radial equilibrium is not appropriate as an outlet boundary condition. Its imposition, even at some far distant downstream location caused considerable problems with numerical convergence to a steady solution. Therefore, Joo and Hynes[8] suggested a simple, new approach to handle such a complicated boundary condition. The calculation domain is imagined to be terminated at the downstream end by a gauze-honeycomb. This was chosen since a gauze-honeycomb is an almost realisable device which will turn the flow at each radial and circumferential position to the axial direction. The static pressure downstream of the honeycomb will thus be uniform. The gauze-honeycomb also has throttle-like pressure drop characteristics and this might be expected to have a benign effect on the transient aspect of the convergence process. The presence of such a device will, of course, affect the flow upstream of the outlet boundary, so that the outlet boundary should still extend to a sufficient length downstream of the fan to ensure that the flow through the rotor itself is not affected. A detailed description of the implementation of this outlet boundary condition into numerical scheme is found in Joo and Hynes [4].

The calculations are performed for an engine operating at 95% of design fan speed where the total pressure ratio is about 1.68 and the mass flow is 916 kg/s and the bypass ratio is 4.51. A $27 \times 121 \times 19$ finite volume grid is used. The calculation results are compared with the total pressure measured using a number of rakes mounted near the leading edge of the OGV and ESS in Fig.2 (Joo and Hynes [6]).

The values shown in the figure are percentage variations about the mean representing the average value at that particular radius, as,

$$\frac{P_0(r,\theta) - \overline{P_0}(r)}{\overline{P_0}(r)} \times 100\ (\%) \qquad (2)$$

The figure shows that the calculation results are in good agreement with the experimental data for both the level and pattern of the variation. The major difference between the two results is in the angular position; the predicted flow field is shifted by

about 30°in the opposite direction to fan rotation relative to the measurements. The neglect of unsteadiness, which causes the time lag response of the fan, in framing the rotor actuator disk boundary conditions is a possibility, as is the modeling of the entire core section of the engine by a boundary condition. The shift in angular position is, also, due to the actuator disk model with zero length that cannot consider a particle path within a blade passage. This is the only comparison with experimental data for validation of the method since the experimental data available is limited, but the agreement between the calculated and the measured results in Fig.3 is more than good enough for many engineering purposes. The flow field immediately downstream of the fan and, by inference, the flow field immediately upstream is probably accurate enough, for example, to enable realistic estimates of the circumferential variation in loading on rotor blades to be made for the purposes of fan vibration and noise level assessments.

Both sets of results show that total pressure delivered by the fan has an 11 % variation about the mean value around the annulus at the tip and 8% at the hub. This asymmetry of total pressure rise is caused by the effects of asymmetric inlet geometry combined with the upstream effects of the core engine and the pylon. Therefore, the characteristics of only the interaction between drooped intake and fan flow fields are investigated and described in the following section.

DROOPED INTAKE AND FAN FLOW FIELD INTERACTION IN CIVIL TURBOFAN ENGINE

To investigate the characteristics of the interaction between drooped intake and fan flow fields, calculations have been performed for the drooped intake and fan flow fields where all components downstream of the fan are removed. In addition, the calculation for the duct alone with no fan present was performed to see the upstream flow redistribution due to the presence of the fan. In the both calculations, the throttle-like boundary condition is applied at the outlet boundary to the calculation domain. The 'throttle' coefficient for the calculation of the duct alone was set to give the same mass flow as one for the calculation of the drooped intake with the fan.

The percentage variation of static pressure at the fan actuator disk inlet is shown in Fig.3 for both calculations. The calculation of the duct without the fan shows the symmetric and small static pressure variation. This shows that the large scale non-uniform static pressure field produced by the asymmetric drooped intake becomes uniform as the annulus becomes axisymmetric. On the other hand, the presence of the fan considerably modifies the static pressure field upstream of the fan for both the level and phase of the variation. The circumferential position of the peak value is rotated by about 45°in the opposite direction to fan rotation and the level of non-uniformity is much higher. The effect on the upstream flow redistribution appears more strongly in the hub region than in the tip region. The strength of this effect decays upstream of the fan and is negligible at half a mean radius upstream (Fig.4).

The static pressure variation at the fan face must be accompanied by variations in axial and circumferential velocity because total pressure is uniform upstream of the fan. The resulting changes in flow coefficient and in incidence will produce non-

uniform fan performance at each circumferential and radial position. The percentage variation of total pressure at the fan actuator disk exit is shown in Fig.5-a. The result indicates that the effect of the drooped intake on the fan performance is stronger in the hub region (7% variation) than in the tip region (4% variation).

When compared with the prediction including the combined effects of all components (Fig.5-b), it can be seen that the asymmetry of fan performance is similar in the core section, whilst in the bypass section the total pressure variation due to the drooped intake is small, particularly in the top region. This suggests that the effect of the drooped intake dominates the change of fan performance in the core section, but the flow in the bypass section is more strongly affected by the pylon downstream of the fan.

NON-UNIFORM TOTAL PRESSURE INLET FLOW AND FAN FLOW FILED INTERACTION IN MUTISTAGE TURBOFAN ENGINE

The computational method is secondly applied to the calculation of the flow in a military multistage turbofan engine which is subjected to inlet flow with non-uniform stagnation pressure of 180° square wave type. Fig.6 shows a cross section of calculation domain that is used to model the flow through the multistage turbofan engine and its installation. The engine has an axisymmetric intake and two stage turbofans and a stator.

As in the calculation of the civil turbofan engine, two stage blade rows and the stator downstream are contracted to plane actuator disks which are located at mid-chord of each blade row. The flow fields upstream and downstream of the blade row are found using a fully three-dimensional computational method and coupled by boundary conditions imposed across the actuator disk to represent the blade row performance.

The values of relative flow angles and losses at the exit to the fan actuator disk were obtained from a throughflow calculation for multistage fan operating near design in uniform inlet flow. The calculation domain in the core engine section is extended to downstream of pylon where a boundary condition simulating the presence of the core engine is imposed. The calculation domain in the bypass stream also includes the pylon and a throttle-like boundary condition, as in the calculation of the civil turbofan engine, is applied at the outlet.

The flow at the inlet boundary to the calculation domain is assumed to be non-swirling, to have non-uniform total pressure of 180° square wave type and constant total temperature and to be roughly aligned with the streamwise surfaces of the calculation grid. The magnitude of total pressure distortion is ± 7.5% of mean value. The calculations are performed for an engine operating at design fan speed where the total pressure ratio is about 2.52 and the mass flow is 27.9 kg/s and the bypass ratio is 0.84. A $37 \times 150 \times 21$ finite volume grid is used.

A percentage variation of static pressure at the first rotor actuator disk inlet is shown in Fig.7-a. The static pressure at inlet plane to the intake is constant and would remain constant if the fans do not exist in the duct, but the presence of the fans force

to redistribute the inlet flow significantly. The calculation result shows 20% variation about the mean value around the annulus at the tip and 13% at the hub and around 60° difference of phase angle in the fan rotation direction with total pressure distortion. This significant variation of static pressure is caused by the interaction between non-uniform inlet flow and the first rotor, and shows that the both flow fields are strongly coupled. The effects of the fan on the upstream flow redistribution appears more strongly in hub region than in the tip region, as in the civil engine, and it would be because of the difference between characteristics of pressure rise of rotor blade at hub and at tip. The strength of this effect decays upstream of the rotor, but it is still felt around 55% of magnitude of rotor inlet distortion at half a mean radius upstream (Fig.7-b), and around 35% at a mean radius upstream (Fig.7-c).

The non-uniform inlet flow produces non-uniform fan performance at each circumferential and radial position. Figs. 8 a-e show a percentage of stagnation pressure variations at exits to each blade row. Total pressure variation the first rotor exit has a 14% variation about the mean value around the annulus at the tip and 25% at the hub. This result indicates that inlet total pressure distortion is largely amplified in hub region through the first rotor from 15% variation at the first rotor inlet plane by the strong interaction between non-uniform inlet flow and the first rotor. This non-uniform performance can influence the stall margin of the rotor.

The magnitude of total pressure distortion at the first stator exit is similar to one at the first rotor exit, as it could be expected. It can, also, be seen that total pressure distortion is attenuated through the second rotor from 14% to 10% at tip and from 22% to 15% at hub. This magnitude of total pressure variation remains through the second stator and the third stator. Therefore it can be concluded the features of attenuation of total pressure distortion through the blade row is mainly affected by the characteristic of a rotor which produces work.

It should be noted that the calculation results include the effect of pylon downstream, and, therefore, it is needed to investigate quantitatively the each effect of pylon and non-uniform total pressure inlet.

CONCLUSIONS

One of the important issues in the assessment of the intake/engine compatibility in civil turbofan engines is to predict the coupling effects between the intake and engine. An actuator disk model has been applied to the calculation of the flow through a high bypass ratio turbofan geometry including the effects of the presence of the core support pylon, the core engine and an asymmetric inlet.

In the civil turbofan engine application, the upstream flow field is significantly redistributed by the interaction between the engine and non-uniform inlet static pressure due to the drooped intake. The axial scale over which the upstream flow redistribution takes place is about half a mean radius. The asymmetry in the flow through a modern turbofan is mainly attributed to the drooped intake and the pylon. The pylon has a stronger effect than the drooped intake in the bypass stream section, whilst the droop effect is more important in the core engine section.

In multistage turbofan engine application, also, the upstream flow field is significantly redistributed by the interaction between the engine and non-uniform inlet total pressure. The effect of the multistage fan on the upstream flow redistribution takes place to the distance longer than a mean radius. Therefore, the non-uniform total pressure inlet flow and fan flow field coupling seems to be stronger than the non-uniform static pressure inlet flow and fan flow field coupling. Total pressure distortion is amplified or attenuated through the rotor and the variations of total pressure distortion are little through a stator.

ACKNOWLEDGEMENTS

The author thanks Dr. T.P. Hynes at the Whittle Laboratory, University of Cambridge for his invaluable advice and help to this work. The authors wish to acknowledge support for this study by the Ministry of Science and Technology through National Research Laboratory program.

REFERENCES

[1] Mokelke, H.G., "Prediction Method in Distortion Induced Engine Instability," AGARD Lecture Series, No. 72 (1974).
[2] Dunham, J., "Non-axisymmetric Flows in Axial Flow Compressors," Mechanical Engineering Science Monograph No. 3, pp.1-32 (1965).
[3] Hawthorne, W.R., Mitchell, N.A., McCune, J.E. and Tan, C.S., "Non-axisymmetric Flow through Annular Actuator Discs: Inlet Distortion Problem," ASME Journal of Engineering for Power, Vol. 100, pp.604-617 (1978).
[4] Joo, W.G., and Hynes T.P., "The Simulation of Turbomachinery Blade Rows in Asymmetric Flow Using Actuator Disks," ASME Journal of Turbomachinery, Vol. 119, No. 4, pp.723-732 (1997).
[5] Dawes, W.N., "Development of a 3D Navier-Stokes Solver for Application to All Types of Turbomachinery," ASME Paper 88-GT-70, (1988).
[6] Joo, W.G., and Hynes T.P., "The Applications of Actuator Disks to Calculations of the Flow in Turbofan Installations," ASME Journal of Turbomachinery, Vol. 119, No. 4, pp.733-741 (1997).

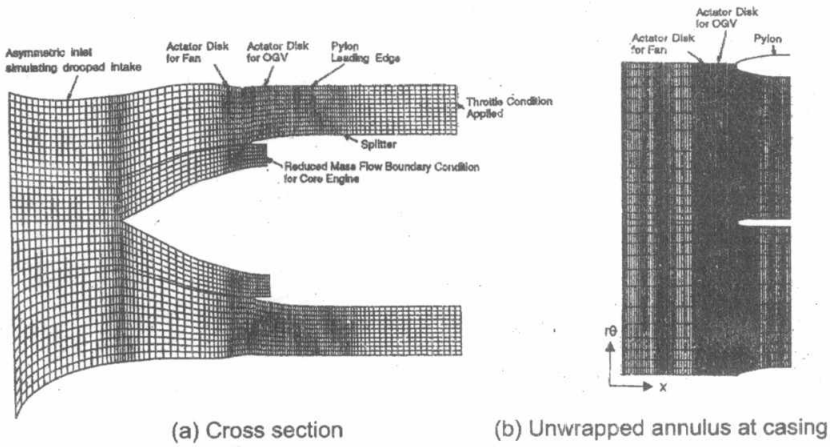

(a) Cross section (b) Unwrapped annulus at casing

Fig.1. Calculation Grids used for predictions of Fan/OGV/Pylon flow field interactions

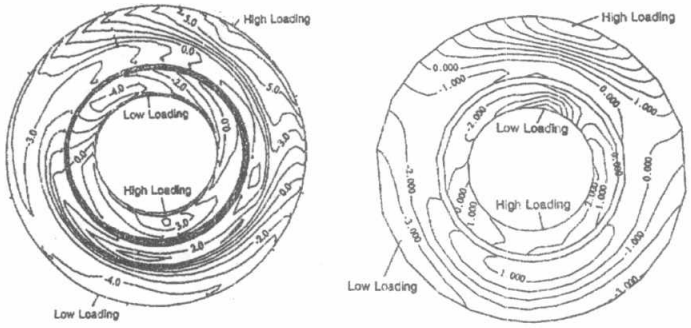

(a) Experiments (b) Prediction

Fig.2. Comparison of measured and predicted circumferential variations in total pressure at OGV inlet downstream of fan operating with inlet simulator (Joo and Hynes [6])

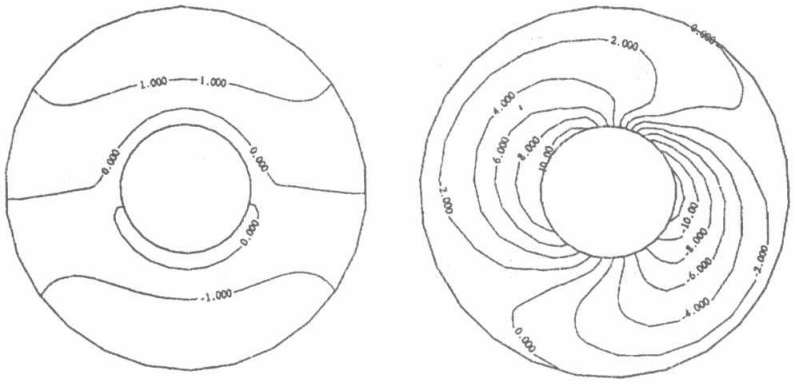

(a) Without Fan (b) With Fan

Fig.3. Comparison of predicted variation(%) of static pressure at fan actuator disk face for drooped inlet with and without the presence of a fan

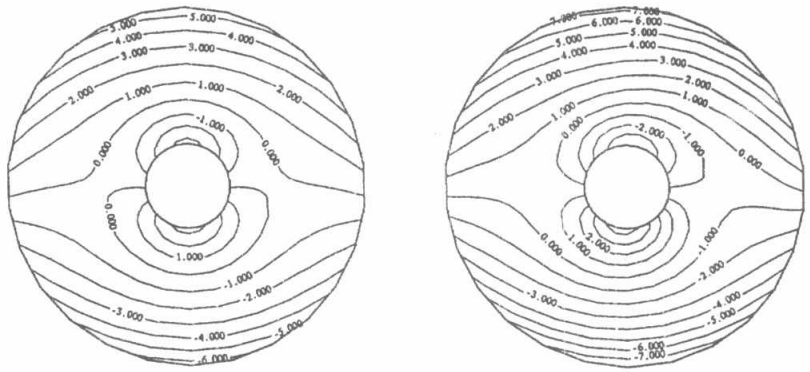

(a) Without Fan (b) With Fan

Fig.4. Comparison of predicted variation(%) of static pressure at half mean radius upstream for drooped inlet with and without the presence of a fan

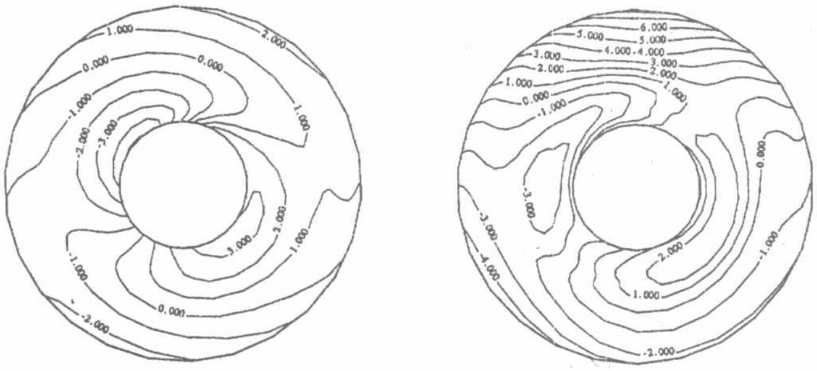

(a) Without all downstream components (b) With all downstream components

Fig.5. Predicted variation of total pressure at fan exit

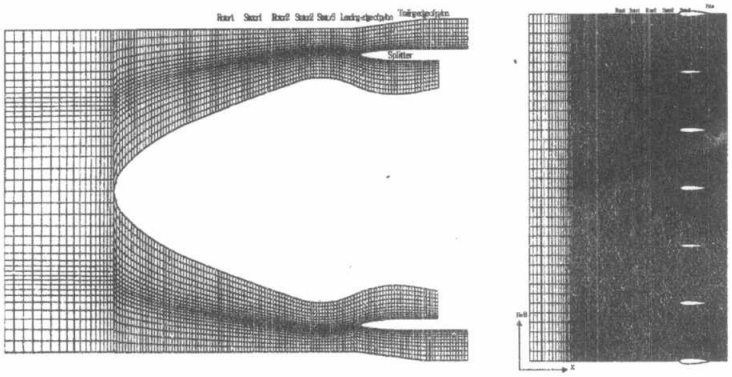

(a) Cross section (b) Unwrapped annulus at mean radius

Fig.6. Calculation Grids for predictions of the non-uniform flow through multistage turbofan engine

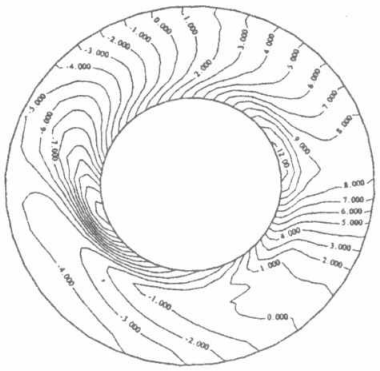

(a) At rotor 1 inlet

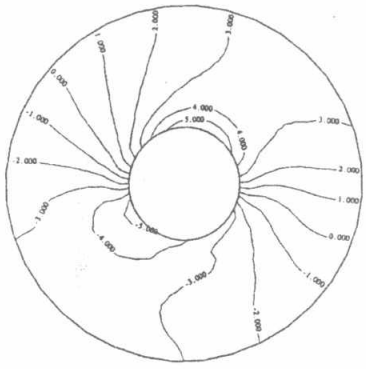

(b) At half mean radius upstream of rotor 1

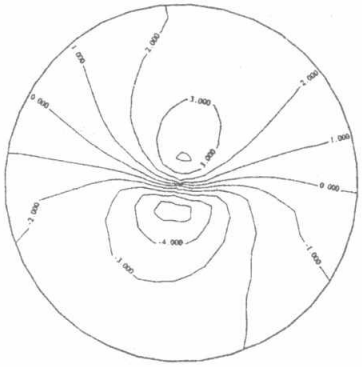

(c) At mean radius upstream of rotor 1

Fig.7. Predicted variation of static pressure

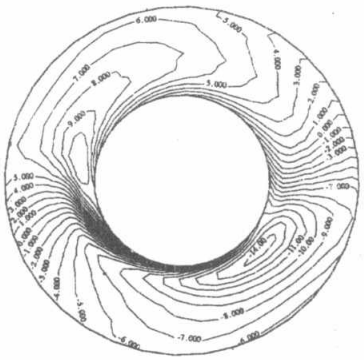

(a) At rotor1 exit

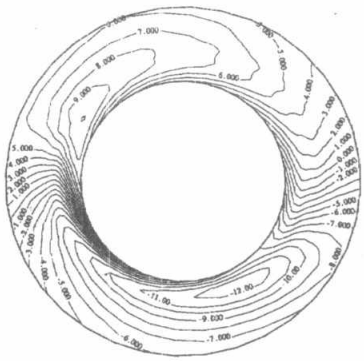

(b) At stator 1 exit

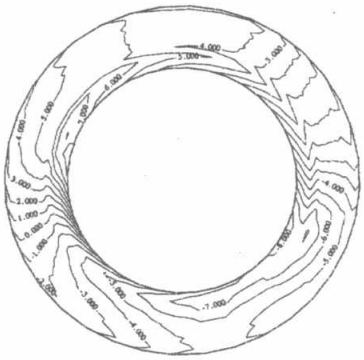

(c) At rotor2 exit

(d) At stator 2 exit

Fig.8. Predicted variation of total pressure (continued)

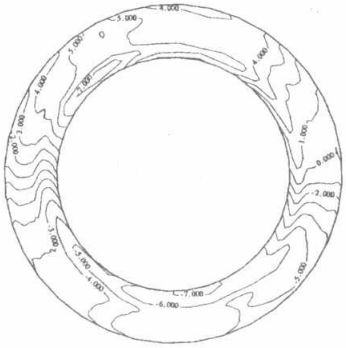

(e) At stator 3 exit

Fig.8. Predicted variation of total pressure (continued)